Molecular Crystals and Liquid Crystals

ISSN: 1542-1406 (Print) 1563-5287 (Online) Journal homepage: http://www.tandfonline.com/loi/gmcl20

Homeotropic Alignment Properties of Liquid Crystal and Photocurable Monomer System via UV Irradiation

Hyo Kang, Jung Min Lee, Jae-Hyun Kim, Jeong-Hun Lee, Jin Seol Park, Jeong Gil Seo & Daeseung Kang

To cite this article: Hyo Kang, Jung Min Lee, Jae-Hyun Kim, Jeong-Hun Lee, Jin Seol Park, Jeong Gil Seo & Daeseung Kang (2015) Homeotropic Alignment Properties of Liquid Crystal and Photocurable Monomer System via UV Irradiation, Molecular Crystals and Liquid Crystals, 606:1, 101-110, DOI: 10.1080/15421406.2014.915637

To link to this article: http://dx.doi.org/10.1080/15421406.2014.915637

Published online: 15 Jan 2015.

Mol. Cryst. Liq. Cryst, Vol. 606: pp. 101–110, 2015

ISSN: 1542-1406 print/1563-5287 online
DOI: 10.1080/15421406.2014.915637

Homeotropic Alignment Properties of Liquid Crystal and Photocurable Monomer System via UV Irradiation

HYO KANG,[1,*] JUNG MIN LEE,[2] JAE-HYUN KIM,[2] JEONG-HUN LEE,[2] JIN SEOL PARK,[2] JEONG GIL SEO,[3] AND DAESEUNG KANG[2]

[1]Materials R&D Center, Samsung Advanced Institute of Technology, Mt. 14-1, Nongseo-dong, Yongin, Gyeonggi-do 446-712, Republic of Korea
[2]Department of Electrical Engineering, Soongsil University, 511 Sangdo-dong, Dongjak-gu, Seoul 156-743, Republic of Korea
[3]Department of Environmental Engineering and Energy, Myongji University, 116 Myongji-ro, Cheoin-gu, Yongin, Gyeonggi-do 449-728, Republic of Korea

We investigated the homeotropic (or vertical) liquid crystal (LC) alignment properties in a LC and photocurable monomer mixture system through UV irradiation. Different homeotropic LC alignment behaviors were observed depending on the type of photocurable monomers and UV irradiation time. The LC alignment behavior showed a good correlation with the wettability of the alignment films due to surface morphology on the alignment layer surfaces by photopolymerization-induced phase separation. The electro-optical characteristics of the LC cells fabricated with these polymer films were as good as or even better than those fabricated from rubbed polyimide (PI) films, the most commonly used LC alignment layers.

Keywords Liquid crystals; optical properties; polymers; thin films

1. Introduction

The mechanical rubbing of polyimide (PI) has been widely studied as a method of fabricating liquid crystal (LC) alignment layers, due to its simplicity and rapidity, where the LCs are aligned parallel to the rubbing direction [1, 2]. However, the rubbing process has disadvantages such as electrostatic discharge, dust generation, and physical damage to the alignment layer surfaces.

Noncontact methods of LC alignment have been investigated in order to overcome the disadvantages of the rubbing method [3–7]. Photoalignment has been taken a notice of promising noncontact alignment methods to be used for the next generation LC displays, including flexible ones, due to its various advantages such as its cleanness, suitability for large substrates, and unrestrictedness to surface morphology. A number of polymers having

*Address correspondence to H. Kang, Tel.: +82 31 8061 1158. E-mail: kangh001@snu.ac.kr; and D. Kang, Tel.: +82 2 820 0642. E-mail: dkang@ssu.ac.kr

Color versions of one or more of the figures in the article can be found online at www.tandfonline.com/gmcl.

various photoreactive groups for photoisomerization, photodimerization, and photodegradation have been studied for photoalignment layers [3, 4, 6].

Generally, homeotropic (or vertical) LC alignment was observed by using PI derivatives having long alkyl or alkyloxy groups, such as semi-flexible copolyimides containing *n*-octadecyl side groups and (*n*-decyloxy)biphenyloxy side groups [8–10]. Recently, homeotropic LC alignment was also achieved by using comb-like polymers, by irradiating photoreactive polymers with UV light, or by fabricating micro and nanostructures [11–17].

Here, we studied a novel method to obtain the homeotropic alignment using LC and photocurable monomer mixture systems, in which the homeotropic alignment was induced on the phase-separated polymer thin film through UV irradiation. Well defined condition for the homeotropic alignment and the electro-optical properties of the novel alignment layers was also included.

2. Experiment

2.1 LC Alignment Process and LC Cell Assembly

We prepared a mixture of a negative dielectric anisotropic LC, MLC-7026-000 (n_e = 1.5577, n_o = 1.4755, and $\triangle\varepsilon$ = –3.7, Merck Co., Pyeongtaek, Korea) and photocurable monomer, NOA61 and NOA65 (Norland Products Inc., Cranbury Township, USA), in a weight ratio of 95 to 5. The LC and photocurable monomer mixtures were infiltrated into empty cells that were made of two indium-tin-oxide (ITO) coated glass substrates separated by 4.5 μm spacers. The LC and photocurable monomer mixture cells were then exposed under an unpolarized UV light for 1, 3, 5, and 10 min at 30 mW/cm^2 ($\lambda\sim$365 nm). Pre-imidized alignment agent (AL60101, Japan Synthetic Rubber Co., Tokyo, Japan) film was fabricated by spin-coating (3000 rpm, 20 sec) onto ITO coated glass substrates. The AL60101 films were prebaked at 70°C for 5 min and then were fully baked at 200°C for 60 min. The polymer films were rubbed using a rubbing machine (RMS-50-M, Nam Il Optical Components Corp., Incheon, Korea). The cells were filled with MLC-7026-000, in isotropic state to avoid creating flow alignment by the capillary action. The manufactured LC cells were sealed with epoxy glue.

2.2 Instrumentation

For scanning electron microscope (SEM) and contact angle measurement, the sample was made by separating ITO coated glass substrates of LC cell and removing the LC on substrates. The contact angles of distilled water on the sample films were determined with a Kruss DSA10 contact angle analyzer equipped with drop shape analysis software. Differential scanning calorimetry (DSC) was carried out on a TA Instruments 2910 Differential Scanning Calorimeter. The heating and cooling rates were 10 °C/min. The T_{ni} are taken at the maxima point (endothermic peaks) in the change in heat capacity with temperature in the DSC thermogram. All thermal transitions were read from reproducible second or later heating scans and first or later cooling scans. The cell gap was measured before filling the LC and photocurable monomer mixture using a spectrophotometer (S2000, Ocean Optics, Dunedin, USA). The polarized optical microscopy (POM) images of the LC cell were taken using an optical microscopy (ECLIPSE E600 POL, Nikon, Tokyo, Japan) equipped with a polarizer and digital camera. Electro-optical properties of the LC cells were investigated using optical apparatus equipped with a He–Ne laser, polarizer, analyzer, and a photodiode detector. The voltage-transmittance (V-T) was measured from the LC cell using the same

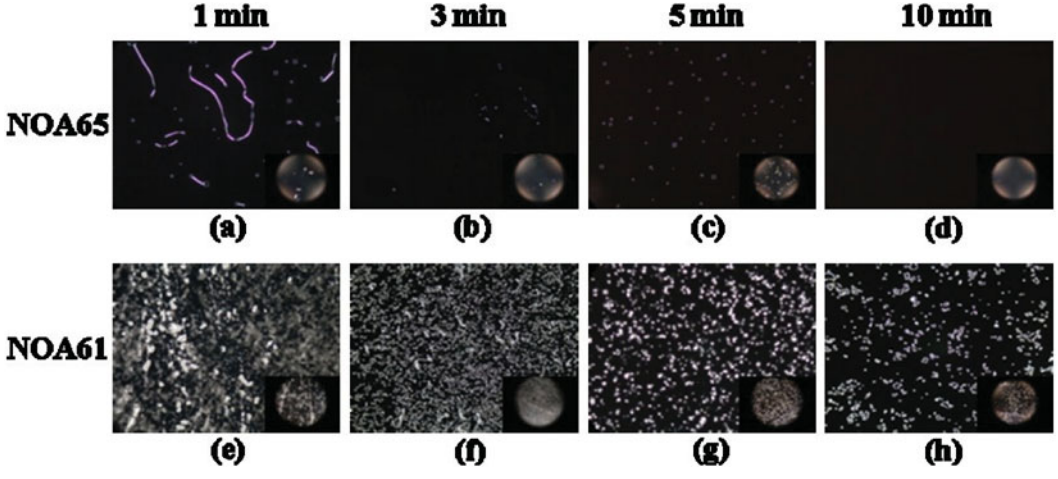

Figure 1. Orthoscopic and conoscopic (inset) POM images of the LC/NOA65 and LC/NOA61 mixture cells with a 95/5 mixture ratio under the following UV irradiation times; 1, 3, 5, and 10 min, respectively.

Figure 2. Orthoscopic and conoscopic (inset) POM images of the LC/NOA65 mixture cells with the LC and NOA65 mixture ratio ranging from (a) 99:1, (b) 97:3, (c) 95:5, (d) 90:10, and (e) 80:20, respectively, under following UV irradiation for 10 min.

method as that reported by others [18, 19]. The threshold voltage (V_{th}) in the V-T curve are defined as the voltages at which the transmittance was increased to 10% of the initial transmittance value [18, 19]. The response times are measured by periodically applying a square voltage (10 V) pulse width different amplitude to the LC cell by an arbitrary waveform function generator (Sony Tektronix, AFG320). The rising (T_r) and falling (T_f) response times for the white-to-black and black-to-white changes, respectively, are defined as the time to transition from 10% to 90% transmittance and vice versa [18, 19]. The total response time (T_t) is determined by the average of T_r and T_f.

3. Results and Discussion

Alignment behavior may be determined according to the nature of the LC and photocurble monomer to be used in the cell. Two commercially available photocurable materials (UV curable polyurethane-related monomers) such as NOA61, NOA65 having nonpolar characteristics were selected in order to obtain the homeotropic LC alignment properties.

Figure 1 shows orthoscopic and conoscopic (inset) POM images of the LC/NOA65 and LC/NOA61 cells with a 95/5 mixture ratio under the following UV irradiation times: 1, 3, 5, and 10 min under UV exposure with an intensity of 30 mW/cm^2 ($\lambda \sim 365$ nm). First of all, at up to 5 min UV exposure, the LC/NOA65 cells showed homeotropic alignment with only a few defects. Uniform homeotropic alignment was not observed during shorter exposure times due to the incomplete photopolymerization. After 10 min, LC/NOA65 cells showed a complete homeotropic alignment without any noticeable defects. However, in the case of the LC/NOA61 mixture cell, the clear homeotropic LC alignment was not observed, because of incomplete phase separation between LC and NOA61 the interfaces. The photoproducts including monomer remained in the bulk LC might become defect image after UV exposure (Figs. 1(e)–(h)). We tried to observe the transition temperature of neat MLC-7026-000, LC in the LC/NOA65 cell after UV irradiation for 10 min, and LC in the LC/NOA61 cell after UV irradiation for 10 min using DSC thermogram. The T_{ni} of the MLC-7026-000 was observed at around 80°C. We could not observe distinct changes of DSC thermogram between the neat MLC-7026-000 and LC in the LC/NOA65 cell after UV irradiation for 10 min. However, in case of the LC in the LC/NOA61 cell, weak endothermic peaks induced by the photoproducts remained in the bulk LC as well as strong endothermic peaks induced by the MLC-7026-000 was observed, respectively.

The POM image of the LC cell made from LC/NOA65 mixture in a weight ratio 99:1, exhibited homeotropic alignment with some defects, as shown in Fig. 2(a). The LC cells fabricated with a weight ratio of 97:3 and 97:5 showed an uniform homeotropic alignment over the whole area, as shown in Figs. 2(b) and 2(c). However, LC cells fabricated with higher photocurable monomer contents (90:10 and 80:20) showed alignment with many

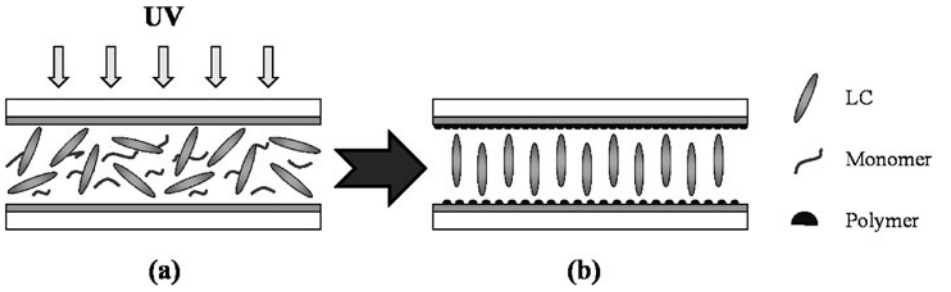

Figure 3. The schematic illustration of homeotropic LC alignment from the phase separated polymer film through UV irradiation; (a) before UV irradiation, (b) after UV irradiation.

defects. In case of the higher photocurable monomer contents, the photopolymerization-induced phase separation generates a fibrillar network and/or elongated domain of the photoproducts in the bulk, which hinders the uniform LC alignment.

Figure 3 illustrates the possible scenario of phase separation of the LC and the photocurable monomer mixed in the isotropic state (Fig. 3(a)). When the LC cell is irradiated using an unpolarized UV light, the photocurable monomer is cured, and the LC/photocurable mixture undergoes photopolymerization-induced phase separation in the vertical direction. The phase separation in the LC/photocurable mixture is believed to be induced by the differences in the surface energy of each component [20, 21]. At a certain UV irradiation condition, a photocured polymer network forms on the substrates and the LC molecules orient vertically from the surface as shown in Fig. 3(b).

The surface morphology and wettability of the film were measured using SEM (Fig. 4) and a contact angle measurement (Fig. 5), respectively, in order to confirm the mechanism of the homeotropic alignment in the LC/photocurable monomer mixture

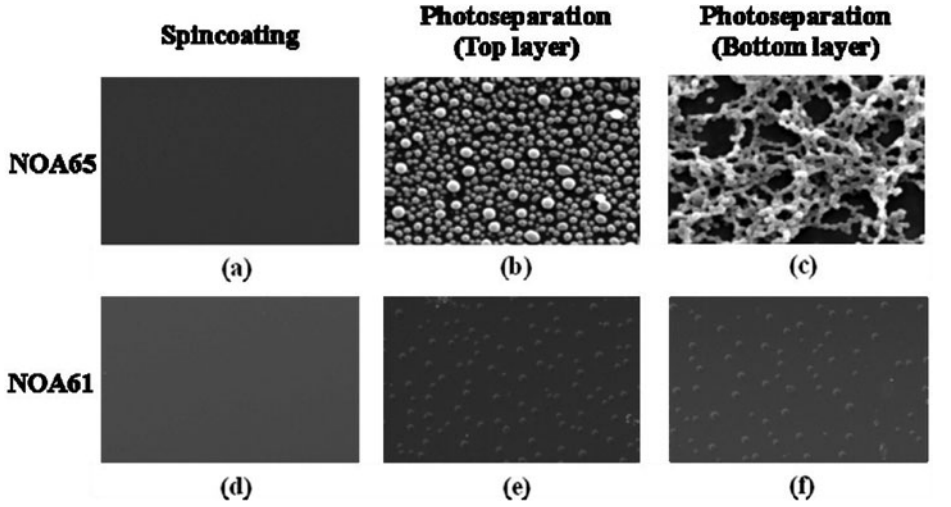

Figure 4. SEM images of the (a) spincoated pure NOA65, the (b) top and (c) bottom substrate of the 95:5 LC/NOA65 mixture cell and (d) spincoated pure NOA61, the (e) top and (f) bottom substrate of the 95:5 LC/NOA61 mixture cell.

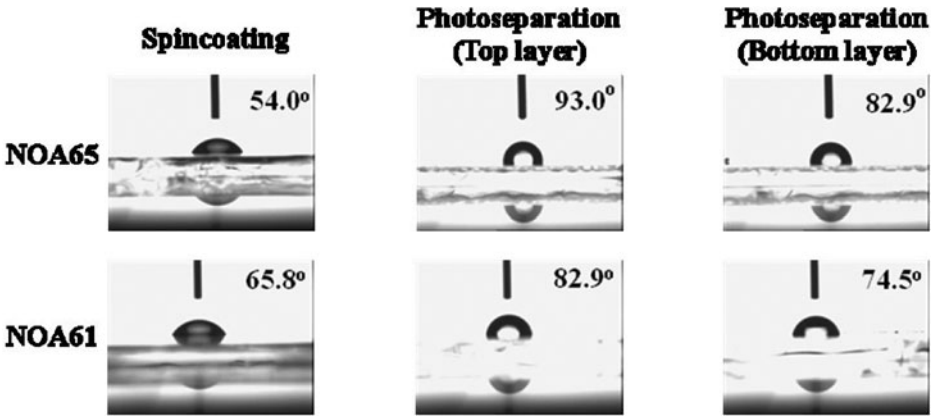

Figure 5. Water contact angle images of the spincoated pure NOA65, the top and bottom substrate of the 95:5 LC/NOA65 mixture cell and spincoated pure NOA61, the top and bottom substrate of the 95:5 LC/NOA61 mixture cell.

cell via phase separation. The top and bottom substrates of the LC cells were carefully separated and the LC on the substrates was selectively removed using solvents. Figures 4(b) and 4(c) show the SEM images of the top and bottom substrate of the LC/NOA65 mixture cell, respectively. In those images, the gravel texture from the phase separated NOA65 can be observed at the top substrate, while the network pattern can be seen at the bottom substrate. However, as shown in SEM images (Figs. 4(e) and 4(f)), sparse gravel texture was observed from the top and bottom substrate of a LC/NOA61 mixture cell due to the incomplete phase separation between LC and NOA61. The photopolymerization rate of thiol−ene-based photocurable monomers such as NOA65 and NOA61 is higher at the region located close to the UV light source. Therefore, more photocurable monomers are reacted at there, generating a gradient of the photocurable monomer concentration, thereby inducing a migration (or diffusion) of the photocurable monomer from the bulk to the irradiated substrates and also a migration of the LC molecules in the opposite direction. We believe that the migration rate difference between the photocurable monomers and LCs affected by the intrinsic properties such as surface tension and viscosity of the each component is important. The migration rate difference between LC and NOA65 was sufficient for complete phase separation and thus gravel and network patterns were observed from the top and bottom substrate of a LC/NOA65 mixture cell, respectively. However, the migration rate difference between LC and NOA61 was insufficient for complete phase separation and thus sparse gravel pattern was observed at both the top and bottom substrates of a LC/NOA61 mixture cell. To compare the surface morphology, we performed a contrast experiment using substrates coated with pure NOA65 and NOA61 film. Figures 4(a) and 4(d) show the surface texture of the substrate of the pure NOA65 and NOA61 film, respectively. As can be seen, the pure NOA65 and NOA61 surfaces are smooth without any noticeable patterns. This SEM results confirm that the gravel and network patterns were obtained through the phase separation process via UV irradiation.

The water contact angle of pure NOA65 film was found to be 54.0° while the water contact angles of the top and bottom substrates of the LC/NOA65 mixture cell were found to be 93.0° and 89.2°, respectively, as shown in Fig. 5. The water contact angle increases by 39.0° and 35.2° in the top and bottom substrates. It has been well known that a low surface energy or low wettability results in high water contact angles [22].

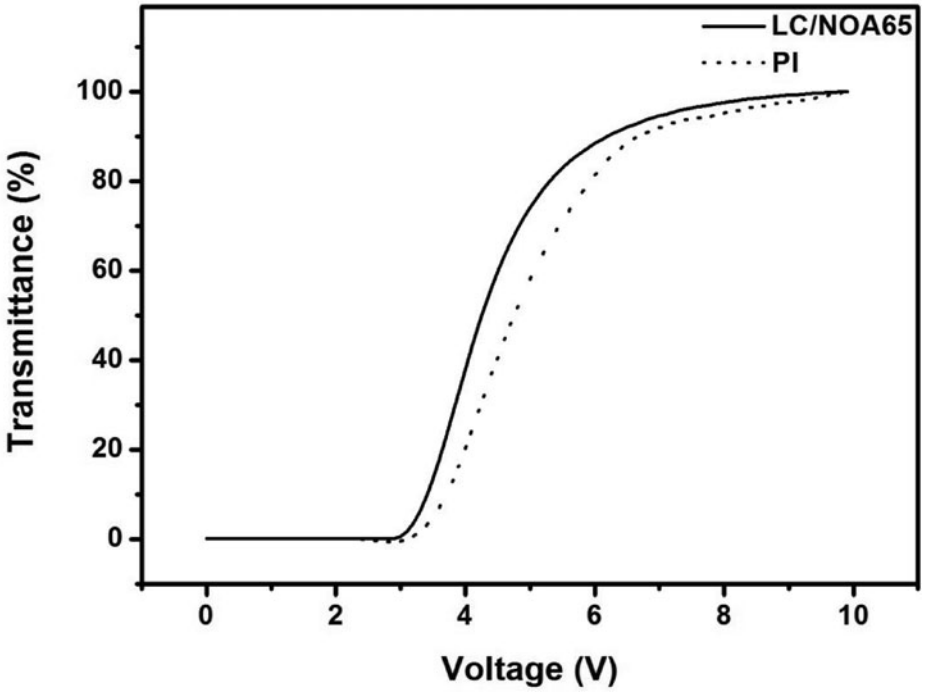

Figure 6. Voltage-transmittance (V-T) curve of the LC cells fabricated using the UV treated LC/NOA65 mixture and rubbed polyimide film.

Generally, the LC molecules are oriented vertically with respect to the substrate if the surface energy of the substrate (γ_s) is smaller than that of LC (γ_L) [23]. In this system, polymer gravel and network patterns resulting from the phase separation of LC/NOA65 mixture via photopolymerization increase the surface roughness and, thereby, induce a higher water contact angle. As a result, homeotropic LC alignment was obtained in the LC/NOA65 cells, where network or gravel morphologies had formed at the substrates due to phase separation. On the other hand, the water contact angle of the substrate of pure NOA61 film was found to be 65.8° while the water contact angles of the top and bottom substrates of the LC/NOA61 mixture cell were found to be 82.9° and 74.5°, respectively. The water contact angle increases by 17.1° and 8.7° in the top and bottom substrates. Conclusively, the substrates of the top and bottom of the LC/NOA61 mixture cell and the pure NOA65, NOA61 film induce random tilted and planar alignment of the LC molecules due to their relatively low water contact angles.

The electro-optical performance of the LC cells fabricated using the UV treated LC/NOA65 mixture cell and rubbed PI film (AL60101 from Japan Synthetic Rubber Co., Ltd.) was determined by measuring the voltage-transmittance (V-T) curve and response time values using the same condition (Fig. 6 and Table 1). In this study, same nematic LC with a negative dielectric anisotropy, MLC-7026-000, which shows a suitable switching behavior for vertical alignment (VA) mode, was used. At first, we measured the pretilt angles of the LC cells made from LC/NOA65 mixture and rubbed PI film. The pretilt angles about 90° and 89.5° of the LC cells made from LC/NOA65 mixture and rubbed PI film was observed, respectively. The LC/NOA65 cell has a lower operating voltage and

Table 1. Threshold voltage and response time values of the LC cell

Sample	Threshold voltage (V) V_{th}	Response time (ms) T_r	T_f	T_t
LC/NOA65	3.4	15	10	12.5
AL60101	3.8	26	12	19

faster response time than those of the LC cell made from the rubbed PI film. For example, the V_{th} value (3.4 V) of the LC/NOA65 mixture cell was lower than those of the LC cell fabricated with the rubbed PI films ($V_{th} = 3.8$ V), possibly due to the anchoring energy effects of the alignment layer surfaces [18, 24] and/or doping effect induced by unreacted photocurable monomer and partially reacted photocured products in LC mixtures [25]. The response times, T_r of 15 ms and T_f of 10 ms, for the LC/NOA65 mixture cell are faster than those, T_r of 26 ms and T_f of 12 ms, for the rubbed PI film, possibly due to the dielectric and anchoring energy effects of the alignment layer surfaces [18, 24] and/or doping effect induced by unreacted photocurable monomer and partially reacted photocured products in LC mixtures [25]. The electro-optical performance of the LC cell from the UV treated LC/NOA65 mixture was as good as or even better than that from the rubbed PI film, which suggests that these novel alignment films can be used for LC display applications. Therefore, we believe that these polymer films can be good candidates as an alignment layer for flexible LC display applications, such as VA mode.

The thermal stability of the LC cells made from the LC/NOA65 mixture was estimated from the POM images after heating the LC cell for 10 min at various temperatures, such as 100, 150, 200, and 250°C, respectively (Fig. 7). The POM images of the LC cells fabricated with these films indicate that the homeotropic LC aligning ability was maintained when heated for 10 min at 250°C. Therefore, the processing temperature of this polymer for LCD applications should be below 250°C.

Recently, considerable effort has been made to develop plastic substrates for flexible LC displays [26]. All of the LC cells made from the LC/NOA65 mixture on PET (polyethylene terephthalate) substrates exhibit similar LC alignment behavior compared with the LC cells made from same alignment films on ITO substrates as previously shown in Fig. 1. We

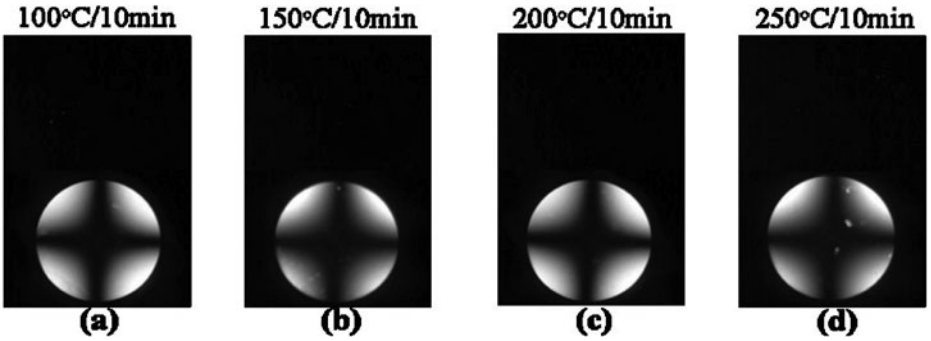

Figure 7. POM images of the UV treated LC/NOA65 mixture cells with annealed for 10 min at (a) 100°C, (b) 150°C, (c) 200°C, and (d) 250°C.

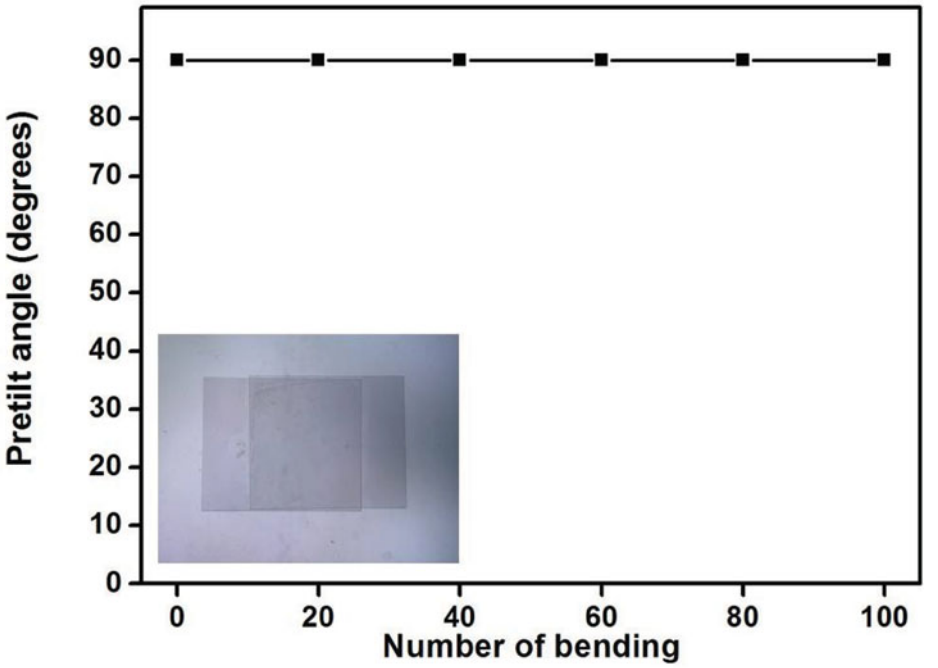

Figure 8. Pretilt angles of the UV treated LC/NOA65 mixture cells on PET substrate as a function of number of bending.

found that the LC cells fabricated using the phase separated NOA65 films on plastic PET substrates show homeotropic LC alignment behavior. For example, the photo images of the LC cell made from the NOA65 film on the PET substrate clearly show homeotropic LC alignment behavior (inset image of the Fig. 8). Furthermore, this LC cell showed very nice homeotropic LC aligning ability with a high pretilt angle of about 90° which was maintained after bending it 100 times (Fig. 8). Therefore, these films can be considered as candidate LC alignment layers for flexible LC displays, such as in VA mode applications.

4. Conclusions

A novel method for the homeotropic (or vertical) LC alignment in the LC and photocurable monomer mixture cell by using the UV irradiation was investigated. We observed the alignment transition of the cells by varying the mixing ratio of LC/photocurable monomer and UV irradiation time and photocurable type. We also found that surface morphology plays an important role in the formation of the homeotropic LC alignment. The homeotropic LC alignment behavior was correlated well with the wettability of the alignment films due to the surface morphology such as gravel and network patterns on the alignment layer surfaces by photopolymerization-induced phase separation. Good electro-optical properties were observed for the cells made from the LC and photocurable monomer mixture. For example, the V_{th} and response time of these LC cell were 3.4 V and 12.5 ms, respectively, indicating that these LC cells were similar to those fabricated from rubbed PI films. Therefore, these novel methods provide great potential for application in flexible LC devices using vertically aligned LCs.

Acknowledgments

This work was supported by the Advanced Track of Green Production Processing for Reducing Greenhouse Gas Emission of the Korea Institute of Energy Technology Evaluation and Planning(KETEP) grant funded by the Korea government Ministry of Knowledge Economy (No. 20114010203140). Authors express their gratitude to Prof. J.-C. Lee at Seoul National University for useful discussions.

References

[1] Kohki, T., Masaki, H., Mitsuhiro, K., Nobuyuki, I., Ray, H., & Masanori, S. (2005). In: *Alignment Technologies and Applications of Liquid Crystal Devices*, Gray G. W., Goodby J. W., & Fukuda A., (Eds.), Taylor & Francis: New York, 7.
[2] Ghosh, M. K., & Mittal, K. L. (1996). *Polyimides: Fundamentals and Applications*. Marcel Dekker: New York.
[3] Ichimura, K. (2000). *Chem. Rev.*, *100*, 1847.
[4] O'Neill, M., & Kelly, S. M. (2000). *J Phys D: Appl Phys*, *33*, R67.
[5] Schadt, M. (1997). *Annu. Rev. Mater. Sci.*, *27*, 305.
[6] Almeria, N., & Paul, R. (2002). *Chem. Rev.*, *102*, 4139.
[7] Lee, H.-J. *et al.* (2011). *Mater. Chem. Phys.*, *126*, 628.
[8] Lee, S. W. *et al.* (2000). *Mol. Cryst. Liq. Cryst.*, *349*, 279.
[9] Lee, Y. J., Kim, Y. W., Ha, J. D., Oh, J. M., & Yi, M. H. (2007). *Polym. Adv. Technol.*, *18*, 226.
[10] Lee, S. B., *et al.* (2006). *Polymer*, *47*, 6606.
[11] Kang, H., Sohn, E.-H., Kang, D., & Lee, J.-C. (2009). *Liq. Cryst.*,*36*, 855.
[12] Kang, H., Park, J. S., Kang, D., & Lee, J.-C. (2009). *Polym. Adv. Technol.*,*20*, 878.
[13] Kang, H., Kim, T.-H., Kang, D., & Lee, J.-C. (2009). *Macromol. Chem. Phys.*, *210*, 926.
[14] Zhao, D. *et al.* (2009). *J. Phys. Chem. B*, *113*, 2961.
[15] Park, H. G. *et al.* (2011). *Soft Matter*, *7*, 5610.
[16] Gwag, J. S. *et al.* (2008). *Nanotechnology*, *19*, 395301.
[17] Lee, K., Kang, H., Lee, J.-C., Kang, D., & Shin. K., (2011). *Liq. Cryst.*, *38*, 1131.
[18] Wu, S.-T., & Yang, D.-K. (2001). *Reflective Liquid Crystal Displays.* John Wiley & Sons: West Sussex.
[19] Boer, W. D. (2005). *Active Matrix Liquid Crystal Displays: Fundamental and Applications*. Elsevier: Amsterdam.
[20] Xu, Z. *et al.* (2009). *Adv. Funct. Mater.*, *19*, 1227.
[21] Ma, H. *et al.* (2011). *Langmuir*, *27*, 1056.
[22] Owens, D. K., & Wendt, R. C. (1969). *J. Appl. Polym. Sci.*, *13*, 1741.
[23] Kahn, F. J., Taylor, G. N., & Schonhor, H. (1973). *Proc. IEEE.*, *61*, 823.
[24] Jia, M., Ge, Z., Song, Q., & Wu, S.-T. (2008). *Appl. Phys. Lett.*, *92*, 061102/1.
[25] Lee, W.-K. *et al.* (2013). *Nanoscale*, *5*, 193.
[26] MacDonald, B. A. *et al.* (2005). In: *Flexible Flat Panel Displays*, Crawford, G. P. (Ed.): John Wiley & Sons: West Sussex, 26.